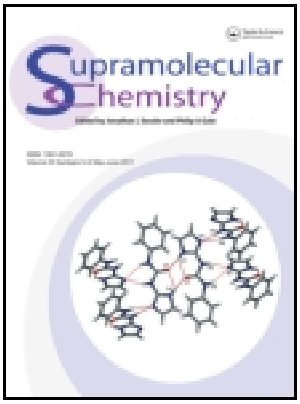

Supramolecular Chemistry
Publication details, including instructions for authors and subscription information:
http://www.tandfonline.com/loi/gsch20

Pyrene-based simple new hetero bis amide pyridinium salt for selective sensing of benzoate and hydrogen sulphate

Kumaresh Ghosh [a] & Avik Ranjan Sarkar [a]
[a] Department of Chemistry, University of Kalyani, Nadia, Kalyani, 741235, India
Published online: 10 May 2011.

Supramolecular Chemistry
Vol. 23, No. 5, May 2011, 365–371

Taylor & Francis
Taylor & Francis Group

Pyrene-based simple new hetero bis amide pyridinium salt for selective sensing of benzoate and hydrogen sulphate

Kumaresh Ghosh* and Avik Ranjan Sarkar

Department of Chemistry, University of Kalyani, Nadia, Kalyani 741235, India

(*Received 8 March 2010; final version received 7 August 2010*)

A new pyrene-based hetero bis amide pyridinium salt **1** has been designed and synthesised. The hetero bis amide salt **1** selectively recognises benzoate over a range of aliphatic monocarboxylates in $CHCl_3$ containing 2% CH_3CN by showing concomitant increase in emission of pyrene. The flexible cleft of **1** also showed selective sensing of tetrahedral-shaped HSO_4^- ion over $H_2PO_4^-$ ion. The recognition property of **1** was evaluated by ^1H NMR, UV–vis and fluorescence studies.

Keywords: benzoate recognition; hydrogen sulphate recognition; pyrene-based receptor; pyridinium salt; anion recognition

The rational design of molecules that exhibit selective recognition of anion by showing change in fluorescence has gained much interest over the past decade (*1–4*). Anion-induced changes in fluorescence appear to be particularly attractive in anion recognition due to the simplicity and high detection limit of fluorescence (*5–8*). In devising these sensors, various functional sites with hydrogen bond donors and acceptors are usually installed in close proximity to the fluorophore. Moreover, to gain selectivity in the recognition process by this class of receptors, size and shape matching between the receptor and substrate is crucial. In addition, anions are prone to interact through either electrostatic or hydrogen bond interactions and thus the incorporation of positively charged groups [ammonium (*9*), guanidinium (*10*), pyridinium (*11*), benzimidazolium (*12–14*) and imidazolium (*15*)] along with neutral hydrogen bond donors [amide (*16*), urea (*17*), pyrrole (*18*), sulphonamide (*19*), etc.] into the designed receptor is fundamentally important. Among the different positively charged species, the pyridinium motif is less explored. To investigate the significance of unconventional C-H- - -O hydrogen bonds in highly polar solvents for carboxylate ion recognition, Jeong and Cho (*20*), for the first time, reported the use of a pyridinium salt. Later on, this pyridinium motif was used by Steed and co-workers (*21*) in the synthesis of tripodal-shaped receptor for selective sensing of Cl^- ion and also by Gong and Hiratani (*22*) in the synthesis of tripodal-shaped sensor for dihydrogen phosphate. During the course of our work on anion binding, we placed this pyridinium motif onto the different scaffolds for fluorometric assessment of specific anion (*23*). In this paper, we report a new hetero bis amide receptor **1**, in which the pyridinium motif and the pyrene fluorophore are attached to semi-rigid isophthaloyl group via amide linkages. The receptor is found to be efficient in selective sensing of benzoate over a range of aliphatic monocarboxylates in $CHCl_3$ containing 2% CH_3CN involving hydrogen bonding, charge–charge and π-stacking interactions altogether. Tetrahedral-shaped anions such as $H_2PO_4^-$, HSO_4^- are also sensed moderately by the flexible cleft of **1**.

The hetero bis amide salt **1** was obtained according to Scheme 1. The hetero bis amide **2** was, initially, synthesised in 45% yield by high-dilution reaction of two different amines with isophthaloyl dichloride in dry CH_2Cl_2. Subsequent reaction of **2** with *n*-butyl bromide in dry CH_3CN under refluxing condition afforded **1** in 77% yield. The compound **1** was characterised by ^1H, ^{13}C NMR and mass analysis.[1]

Prior to the investigation of the recognition properties of **1** in solution, we performed the optimisation of the different conformations of the structure **1** by MM2 method[2] (Supplementary Data). In principle, the hetero bis amide **1** can exhibit different conformations depending on the orientation of the amides (*in–in*, *in–out* and *out–out*) in solution (*24*). Among the several conformations, one *in–in* ($E = -23.0$ kcal/mol) and one *out–out* ($E = -27.1$ kcal/mol) conformers are energetically stable and they are close in energy values (Supplementary Data, Figure S8A). Between these two, *in–in* conformer ($E = -23.0$ kcal/mol) which has the possibility to complex the sterically fitted guest favourably involving the maximum number of hydrogen bonds, was further optimised using density functional theory (*25*) calculations with the B3LYP functional (*26*, *27*) and the basis set 6-311G**, provided by Gaussian 03 (*28*) (Figure 1). As can be seen from Figure 1,

*Corresponding author. Email: ghosh_k2003@yahoo.co.in

ISSN 1061-0278 print/ISSN 1029-0478 online

DOI: 10.1080/10610278.2010.514911
http://www.informaworld.com

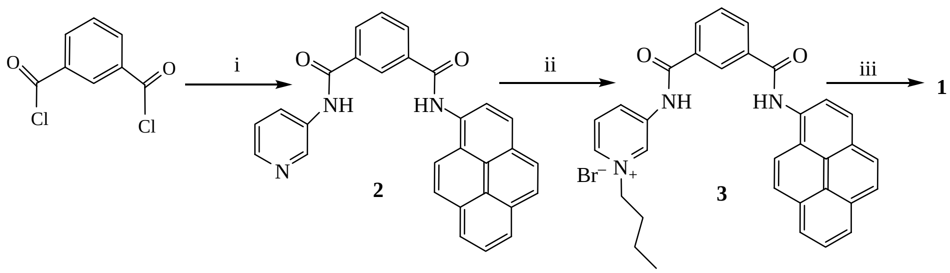

Scheme 1. (i) Dropwise addition of 1-aminopyrene and 3-aminopyridine under high-dilution condition, Et_3N, dry CH_2Cl_2; (ii) *n*-butyl bromide in dry CH_3CN, heating with stirring, 48 h and (iii) NH_4PF_6/aq. MeOH.

the amides are not perfectly in one plane. Pyrene ring is also slightly twisted from the molecular plane and provides a space for the inclusion of anionic guests. To have an idea about the electrophilic character of the receptor, we calculated the global electrophilicity index ($\omega = 0.7946$) of **1** (*29*). The value as determined indicates that the receptor **1** has a significant electrophilic character for the complexation of anionic guests.

Anion-binding properties of **1** with the different anions were investigated in $CHCl_3$ containing 2% CH_3CN by ^1H NMR, UV–vis and fluorescence spectroscopic methods. The fluorescence emission spectra of **1** ($c = 6.11 \times 10^{-5}$ M) were obtained by excitation of the pyrene fluorophore at 340 nm. Figure 2 shows the fluorescence emission changes in compound **1** upon addition of $C_6H_5CO_2^-$, 4-Bu$OC_6H_4CO_2^-$, $CH_3CO_2^-$, $CH_3CH_2CO_2^-$, myristate, salt of ibuprofen, pyridine-3-carboxylate, (*R*)-mandelate, *rac*-lactate, $H_2PO_4^-$, HSO_4^-, ClO_4^- and NO_3^- (10 equiv., tetrabutylammonium salts). As shown in Figure 2, there was a unique change in emission of **1** in the presence of $C_6H_5CO_2^-$ and HSO_4^- ions. In the absence of the guests, the fluorescence emission spectra consisted of a structured and broad band centred at 430 nm, when excited at 340 nm. Upon addition of $C_6H_5COO^-$, the intensity of this band gradually increased with no other spectral changes being observed (i.e. no spectral shifts or formation of new emission bands) (Figure 3). Other aromatic carboxylates such as electron-rich 4-Bu$OC_6H_4CO_2^-$ and electron-deficient pyridine-3-carboxylate upon interaction with **1** also increased emission but to a lesser extent compared to benzoate (Figure 2). Under similar condition, aliphatic mono-carboxylates such as acetate, propanoate, long chain myristate, etc. did not perturb the emission of **1** so markedly (Supplementary Data). The emission of **1** was found to be totally unperturbed in the presence of more steric carboxylate salt such as salt of ibuprofen (Supplementary Data), where the phenyl ring of ibuprofen can experience π-stacking interaction with pyrene. Due to similar steric reason, *rac*-lactate, mandelate also interacted weakly. Interestingly, NO_3^- ion being planar like carboxylate ion, was non-interacting in the binding process. We, additionally, investigated the interaction of **1** with carboxylic acids such as acetic, propanoic, myristic, benzoic, ibuprofen, *rac*-lactic and (*R*)-mendalic acids, which weakly perturbed the emission of **1** (Supplementary Data). In comparison to the planar carboxylate ions, tetrahedral-shaped anion, HSO_4^- only increased the emission (Supplementary Data) significantly. In the presence of 1 equiv. amount of $H_2PO_4^-$, the emission of

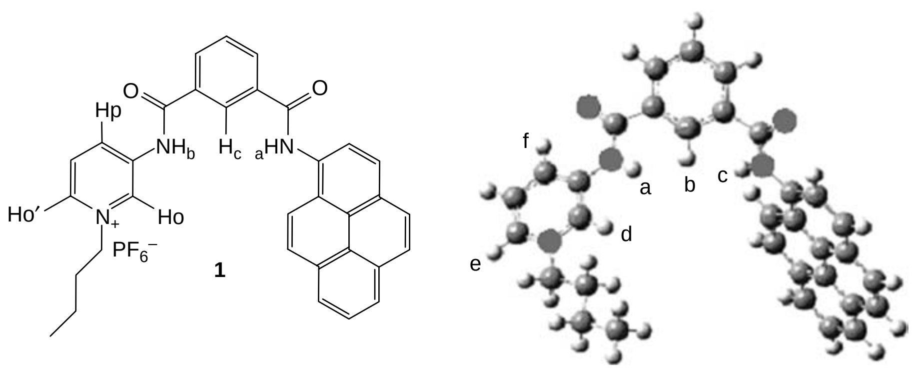

Figure 1. Density functional theory-optimised structure of **1** ($E = -1589.33$ au; atomic charges: $a = 0.2485$, $b = 0.0735$, $c = 0.2314$, $d = 0.1707$, $e = 0.1669$, $f = 0.1902$, $N^+ = -0.3792$).

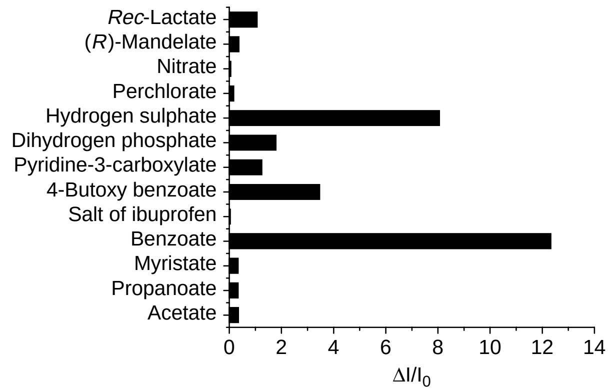

Figure 2. Fluorescence ratio ($I_0 - I/I_0$) of receptor **1** at 407 nm upon addition of 10 equiv. of a particular guest in $CHCl_3$ containing 2% CH_3CN ($c = 6.11 \times 10^{-5}$ M).

1 increased to a small extent. Further addition shifted the band to the longer wavelength with a broad emission at ~500 nm (Figure 4). This broad emission, presumably, is due to the formation of intermolecular excimer upon complexation of $H_2PO_4^-$. All the anions except $H_2PO_4^-$ bind in 1:1 stoichiometric fashion, confirmed by Job's plots (*30*). Figure 5, for example, demonstrates the Job plot for **1** with $C_6H_5CO_2^-$. Even, the linear nature of the fluorescence titration curves for all the anions except $H_2PO_4^-$ in Figure 6 corroborates the 1:1 stoichiometry of the complexes in solution. Receptor **1** binds $H_2PO_4^-$ initially in 1:1 stoichiometry and then attains a 2:1 (host:guest) stoichiometry when excess concentration of the guest is added. The fluorescence enhancing effect of **1** upon complexation of anions can be due to the deactivation of photo-induced electron transfer (PET) process occurring in between the binding site and excited state of pyrene. The large fluorescence enhancing effect of **1** in the presence of $C_6H_5CO_2^-$ over the aliphatic monocarboxylates in the present study is due to the combining effect of hydrogen bonding (both conventional and unconventional), charge–charge and π-stacking interactions for which the PET process is effectively stopped. In relation to this, the different equilibrium binding modes (**A** and **B**) of $C_6H_5CO_2^-$ ion into the diamide core of **1** are suggested in Figure 7. Molecular modelling was performed on these two different modes and interestingly, mode **A** was found to be favourable over mode **B** (Supplementary Data). However, similar binding involving no π-stacking interaction is plausible with aliphatic monocarboxylates. Thus, the contribution of this weak force in the present case discriminates benzoate from

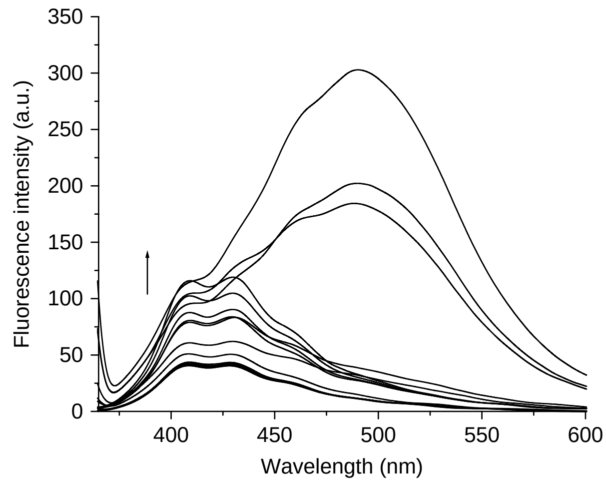

Figure 4. Change in emission of **1** ($c = 6.11 \times 10^{-5}$ M) upon gradual addition of $H_2PO_4^-$ ions in $CHCl_3$ containing 2% CH_3CN.

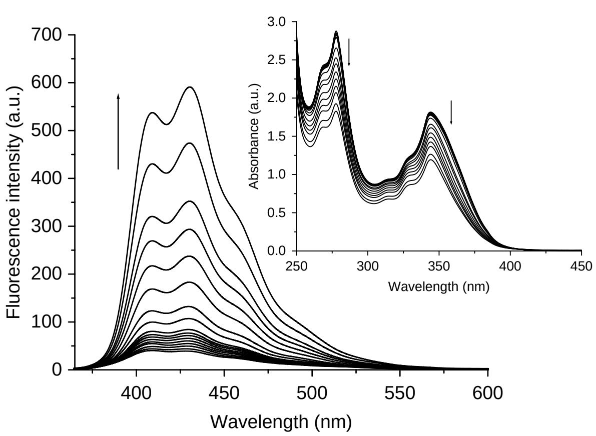

Figure 3. Change in emission of **1** ($c = 6.11 \times 10^{-5}$ M) upon gradual addition of benzoate ions in $CHCl_3$ containing 2% CH_3CN; inset: UV–vis titration spectra of **1** ($c = 6.11 \times 10^{-5}$ M) upon titration with benzoate (10 equiv.) in $CHCl_3$ containing 2% CH_3CN.

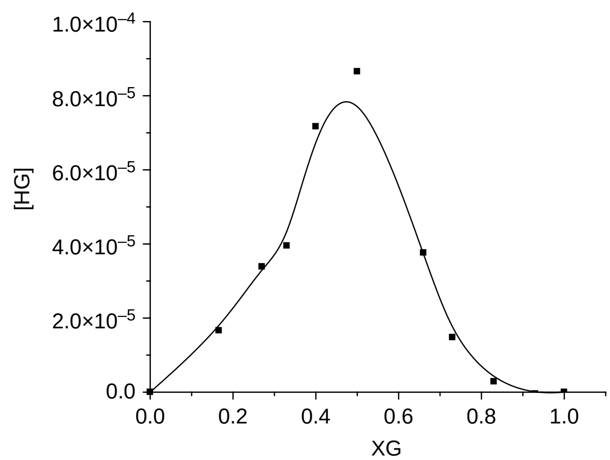

Figure 5. Fluorescence Job's plots of **1** with $C_6H_5CO_2^-$ at 407 nm in $CHCl_3$ containing 2% CH_3CN.

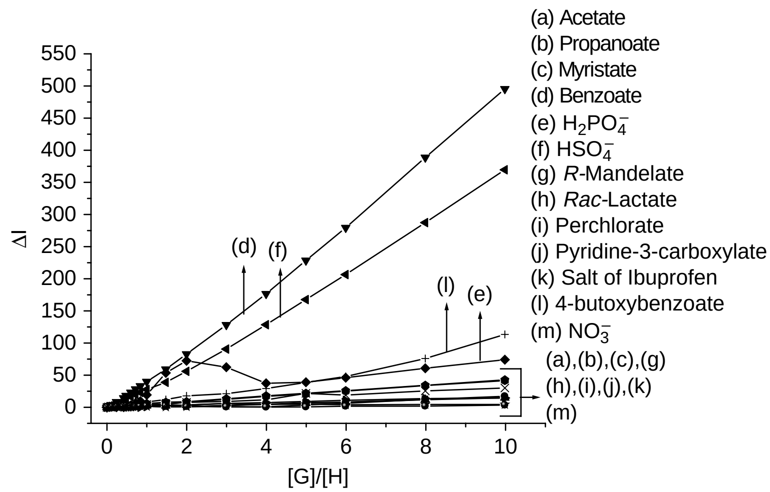

Figure 6. Plot of change in emission of **1** at 407 nm vs. the ratio of guest-to-host concentration.

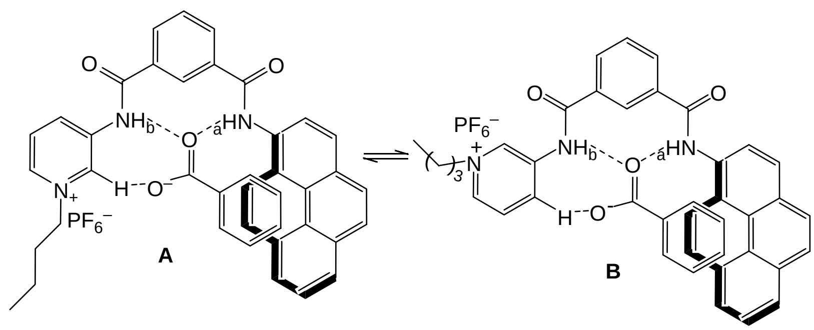

Figure 7. Suggested mode of binding of $C_6H_5CO_2^-$ into the cleft of **1**.

aliphatic monocarboxylates. This has a strong relevance in the distinction between aromatic and aliphatic monocarboxylates. On the other hand, steric fit of the tetrahedral-shaped HSO_4^- ion over $H_2PO_4^-$ and ClO_4^- (less basic compared to organic carboxylates) into the non-planar diamide cleft of **1** induced a marked change in the emission, although there was no role of π-stacking interaction.

To look into the ground state interaction properties, UV–vis titrations of **1** with all the anions in $CHCl_3$ containing 2% CH_3CN were performed. The absorption spectrum of **1**, consisting of bands at 268, 278 and 344 nm, was affected upon addition of all the anions studied. Upon complexation, the intensity of the absorption bands decreased marginally up to the addition of 1 equiv. amount of each anion. Excess addition caused substantial decrease in intensity. The stoichiometries of complexes in the ground state were also found to be 1:1, confirmed by UV Job's plots (Supplementary Data) as well as from the break of the titration curves at [G]/[H] = 1 (Supplementary Data). The change in absorbance of **1** upon titration with $C_6H_5CO_2^-$ ions is displayed in the inset of Figure 3.

Table 1. Binding constant values for **1** in $CHCl_3$ containing 2% CH_3CN.

Guest	K_a (M^{-1})[a]	K_a (M^{-1})[b]
Acetate	[c]	2.49×10^2
Propanoate	[c]	1.91×10^2
Myristate	[c]	1.67×10^2
Benzoate	3.46×10^3	1.32×10^3
4-Butoxybenzoate	8.69×10^2	[c]
Pyridine-3-carboxylate	5.48×10^2	[c]
Ibuprofen salt	[c]	[c]
Nitrate	[c]	[c]
Dihydrogen phosphate	[c]	4.79×10^2
Hydrogen sulphate	1.87×10^3	1.23×10^3
Perchlorate	[c]	1.82×10^2
Rac-Lactate	[c]	2.72×10^2
(*R*)-Mandelate	[c]	3.37×10^2

[a] Determined by the fluorescence method at the wavelength of 407 nm.
[b] Determined by UV–vis method at the wavelength of 344 nm.
[c] Association constants were not determined due to minimum and irregular changes.

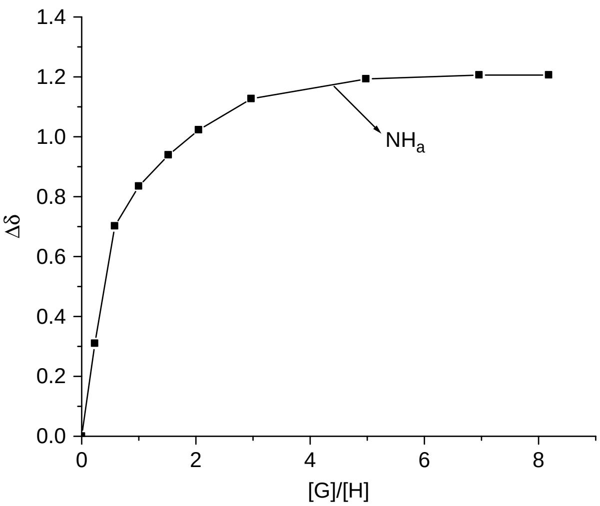

Figure 8. Titration curve for **1** ($c = 1.86 \times 10^{-3}$ M) with tetrabutylammonium salt of benzoate.

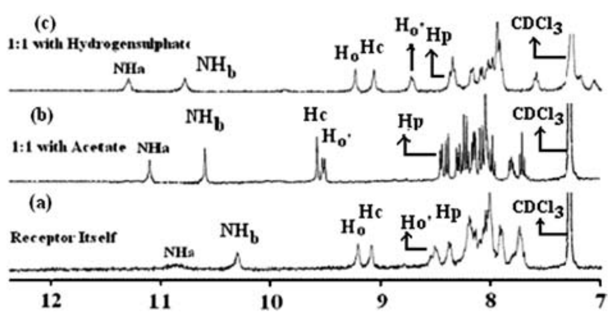

Figure 9. Partial ^{1}H NMR of (a) **1** ($c = 1.86 \times 10^{-3}$ M) and its 1:1 complexes with (b) $C_6H_5COO^-$ N^+Bu_4, (c) CH_3COO^- N^+Bu_4 and (d) HSO_4^- N^+Bu_4 in $CDCl_3$ containing 2% CD_3CN (see labelled structure **1**).

In order to understand the binding selectivity of **1** for the anions, fluorescence and UV–vis titration data were used to calculate the binding constant values (Table 1) (*31*). It is evident from Table 1 that receptor **1** exhibits greater selectivity for aromatic monocarboxylates over the aliphatic monocarboxylates and in the present case especially for $C_6H_5CO_2^-$ ion accompanying with a higher binding constant value. The electron-rich and electron-deficient aromatic monocarboxylates such as 4-$BuOC_6H_4CO_2^-$ and pyridine-3-carboxylate, respectively, exhibited moderate binding constant values and they were found to be less in magnitude than $C_6H_5CO_2^-$. We determined the binding constant value for $C_6H_5CO_2^-$ by the NMR titration method (*32*) at the concentration of $\sim 10^{-3}$ M of **1** and it was found to be $3.99 \times 10^3\,M^{-1}$ which is higher than the value $1.32 \times 10^3\,M^{-1}$ determined by the UV method at the concentration range of $\sim 10^{-5}$ M. In addition, the binding constant values in Table 1 reveal that the selectivity of **1** is found to be slightly higher in the excited state possibly for more polar character of the receptor in the excited state. Based on steric fit, HSO_4^- also shows a greater binding constant value like $C_6H_5CO_2^-$ ion. In this context, it is mentionable that it was difficult to determine the binding constant values for the carboxylic acids with **1** due to a minor change in emission as well as absorption of **1**.

The interaction of **1** with $C_6H_5CO_2^-$ and HSO_4^- was further established by ^{1}H NMR. Pyrene amide proton H_a ($\Delta\delta = 0.84$ ppm) of **1** underwent a downfield chemical shift upon complexation of benzoate (Figure 8). The pyridinium amide proton H_b became broad and difficult to identify. Moreover, in the interaction process, the pyridinium amide arm of **1** was found to be deeply involved in the binding of $C_6H_5CO_2^-$ as proved by large downfield chemical shift of the pyridinium *ortho* proton H_o ($\Delta\delta = 0.92$ ppm) (for titration spectra see Supplementary Data). During interaction, the isophthaloyl *peri* proton H_c also moved to the downfield direction. The protons H_o, $H_{o'}$ and H_p of the pyridinium ring were identified from the analysis of COSY spectrum of **1** (Supplementary data). On the other hand, as can be seen from Figure 9, AcO^- being smaller in size as well as more basic than $C_6H_5CO_2^-$, also showed a downfield shift of the amide protons ($\Delta\delta_{H_a} = 0.20$ ppm; $\Delta\delta_{H_b} = 0.26$ ppm). The *ortho* proton H_o vanished, presumably, due to deprotonation, and the

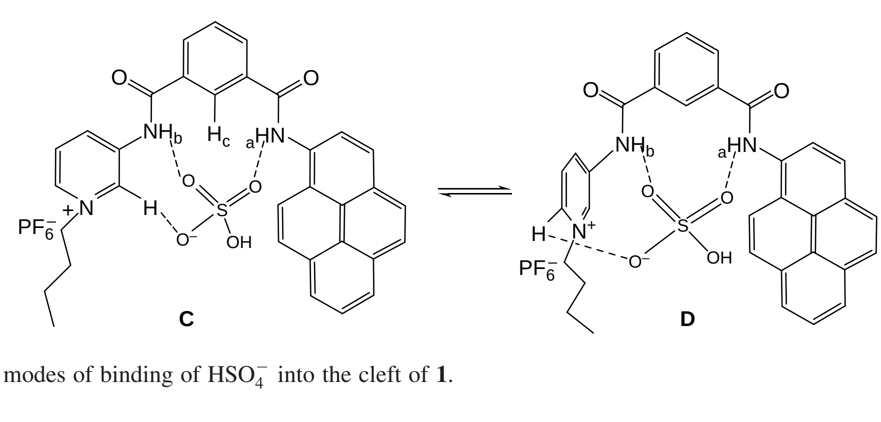

Figure 10. Possible modes of binding of HSO_4^- into the cleft of **1**.

proton assigned as $H_{o'}$ moved to the downfield direction ($\Delta\delta = 0.94$ ppm) effectively. This was also true for HSO_4^- where the amide protons underwent appreciable downfield chemical shift ($\Delta\delta_{H_a} = 0.42$ ppm; $\Delta\delta_{H_b} = 0.48$ ppm) but pyridinium *ortho* proton (H_o) was almost positionally unaffected. The $H_{o'}$ proton moved to the downfield direction weakly suggesting equilibrium binding structures **C/D**, shown in Figure 10. The H_p proton did not show any measurable shift in the interaction process.

In conclusion, we have designed and synthesised a simple hetero bis amide salt **1**, which shows unique recognition and sensing properties. The open cleft of **1** discriminates the aromatic monocarboxylates from the aliphatic ones. Results demonstrate that the hetero bis amide salt **1** selectively recognises benzoate from other aromatic and aliphatic monocarboxylates examined in the present study, by exhibiting large binding-induced fluorescence enhancing effect. In addition, tetrahedral-shaped HSO_4^- is also sensed with moderate binding constant value based on steric complementarity and is differentiated from other tetrahedral-shaped anions studied. The high affinity and selectivity of **1** for benzoate are due to the combined effects of semi-rigid structures, charge–charge interactions, involvement of both N-H- - -O and C-H- - -O hydrogen bonds and more specifically π-stacking interaction. Further progress in this direction is underway in our laboratory.

Supplementary Data

Figures showing the change in absorption and fluorescence spectra of **1** in the presence of the anions and monocarboxylic acids, Job's plots of receptor **1** in presence of the $H_2PO_4^-$, HSO_4^-, binding constant curves for **1** with benzoate and hydrogen sulphate, MM2-optimised geometries of the different conformations of **1** and also of the complex **1** benzoate, COSY spectrum of **1**, NMR titration spectra for **1** with benzoate, binding constant curve for **1** with benzoate, general procedures for fluorescence and UV–vis titrations and Job's plot experiments are available online.

Acknowledgements

We thank the CSIR [01 (2240)/08-EMRII], Government of India for financial support. A.R.S. thanks the University of Kalyani for providing a university research fellowship. K.G. thanks the DST and UGC, Government of India for providing facilities in the department under FIST and SAP programs, respectively.

Notes

1. Mp 124°C; ^{1}H NMR (d_6-DMSO 400 MHz): δ 11.50 (s, NH, 1H), 11.03 (s, NH, 1H), 9.59 (s, 1H), 8.82–8.80 (m, 2H), 8.71 (d, 1H, $J = 8$ Hz), 8.49 (d, 1H, $J = 8$ Hz), 8.37–8.27 (m, 4H), 8.24–8.19 (m, 5H), 8.16–8.09 (m, 2H), 7.85 (t, 1H, $J = 8$ Hz), 4.67 (t, 2H, $J = 8$ Hz), 1.94–1.91 (m, 2H), 1.37–1.31 (m, 2H), 0.93 (t, 3H, $J = 7.20$ Hz); ^{13}C NMR (d_6-DMSO, 100 MHz): δ 165.9, 165.7, 139.4 (one carbon unresolved), 135.8, 135.2, 134.9, 133.5, 131.7, 131.5, 131.2, 130.7, 130.4, 129.1, 128.05, 127.7, 127.25, 127.20, 127.02, 126.4, 125.6, 125.4, 125.1, 125.04, 124.9, 124.8, 124.3, 123.7, 122.8, 61.1, 32.7, 18.7, 13.3; FTIR: ν cm^{-1} (KBr): 3397, 1680, 1635, 1654, 1539, 1555, 1504, 1462; *m/z* (ES$^+$): 498.3 $(M - PF_6^- - 2)^+$.
2. Energy optimisation was performed using CS Chem 3D version 10.0.

References

(1) Gale, P.A. *Coord. Chem. Rev.* **2003**, *240*, 191–221.
(2) *Chemical Sensors and Biosensors for Medical and Biological Applications*; Spichiger-Keller, U.S., Ed.; Wiley: Weinheim, Germany, 1998.
(3) Martinez-Manez, R.; Sancenon, F. *Chem. Rev.* **2003**, *103*, 4419–4476.
(4) Gale, P.A.; García-Garrido, S.E.; Garric, J. *Chem. Soc. Rev.* **2008**, *37*, 151–190.
(5) Gale, P.A. *Coord. Chem. Rev.* **2001**, *213*, 79–128.
(6) Gunnlaugsson, T.; Glynn, M.; Tocci, G.M.; Kruger, P.E.; Pfeffer, F.M. *Coord. Chem. Rev.* **2006**, *250*, 3094–3117, and references cited therein.
(7) De Silva, A.P.; Gunartne, H.Q.; Gunnlaugsson, T.; Huxley, A.J.M.; McCoy, C.P.; Rademacher, J.T.; Rice, T.E. *Chem. Rev.* **1997**, *97*, 1515–1566.
(8) Czarnik, A.W. *Acc. Chem. Res.* **1994**, *27*, 302–308.
(9) Bazzicalupi, C.; Bencini, A.; Bianchi, A.; Fusi, V.; Garcia-Espana, E.; Giorgi, C.; Llinares, J.M.; Ramirez, A.; Valtancoli, B. *Inorg. Chem.* **1999**, *38*, 620–621.
(10) Schmuck, C.; Machon, U. *Eur. J. Org. Chem.* **2006**, 4385.
(11) Ghosh, K.; Sarkar, A.R. *Tetrahedron Lett.* **2009**, *50*, 85–88.
(12) Ghosh, K.; Saha, I.; Patra, A. *Tetrahedron Lett.* **2009**, *50*, 2392–2397, and references cited therein.
(13) Wong, W.W.H.; Vickers, M.S.; Cowley, A.R.; Paul, R.L.; Beer, P.D. *Org. Biomol. Chem.* **2005**, *3*, 4201–4208.
(14) Bai, Y.; Zhang, B.-G.; Xu, J.; Duan, C.-Y.; Dang, D.-B.; Liu, D.-J.; Meng, Q.-J. *New J. Chem.* **2005**, *29*, 777–779.
(15) (a) Kim, S.K.; Kang, B.-G.; Koh, H.S.; Yoon, Y.J.; Jung, S.J.; Jeong, B.; Lee, K.-D.; Yoon, J. *Org. Lett.* **2004**, *6*, 4655–4658. (b) Qin, D.-B.; Xu, F.-B.; Wan, X.-J.; Zhao, Y.-J.; Zhang, Z.-Z. *Tetrahedron Lett.* **2006**, *47*, 5641–5643.
(16) (a) Szumna, A.; Jurczak, J. *Eur. J. Org. Chem.* **2001**, 4031–4039. (b) Bates, G.W.; Gale, P.A.; Light, M.E. *Chem. Commun.* **2007**, 2121–2123.
(17) (a) Cho, E.J.; Ryu, B.J.; Lee, Y.J.; Nam, K.C. *Org. Lett.* **2005**, *7*, 2607–2609. (b) Caltagirone, C.; Bates, G.W.; Gale, P.A.; Light, M.E. *Chem. Commun.* **2008**, 61–63.
(18) Sessler, J.L.; An, D.; Cho, W.-S.; Lynch, V.; Marquez, M. *Chem. Commun.* **2005**, 540–542, and references cited therein.
(19) Mammoliti, O.; Allasia, S.; Dixon, S.; Kilburn, J.D. *Tetrahedron* **2009**, *65*, 2184–2195.
(20) Jeong, K.-S.; Cho, Y.L. *Tetrahedron Lett.* **1997**, *38*, 3279–3282.
(21) Wallance, K.J.; Belcher, W.J.; Turner, D.R.; Syed, K.F.; Steed, J.W. *J. Am. Chem. Soc.* **2003**, *125*, 9699–9715.
(22) Gong, W.; Hiratani, K. *Tetrahedron Lett.* **2008**, *49*, 5655–5657.
(23) (a) Ghosh, K.; Sarkar, A.R.; Masanta, G. *Tetrahedron Lett.* **2007**, *48*, 8725–8729. (b) Ghosh, K.; Sarkar, A.R. *Tetrahedron Lett.* **2009**, *50*, 85–88. (c) Ghosh, K.; Sarkar, A.R.; Patra, A. *Tetrahedron Lett.* **2009**, *50*, 6557–6561.

(24) (a) Sessler, J.L.; Barkey, N.M.; Pantos, G.D.; Lynch, V.M. *New J. Chem.* **2007**, *31*, 646–654. (b) Goswami, S.; Ghosh, K.; Dasgupta, S. *Tetrahedron* **1996**, *52*, 12223–12232.
(25) Parr, R.G.; Yang, W. *Annu. Rev. Phys. Chem.* **1995**, *46*, 701–728.
(26) Becke, A.D. *J. Chem. Phys.* **1993**, *98*, 5648–5652.
(27) Lee, C.; Yang, W.; Parr, R.G. *Phys. Rev. B* **1988**, *37*, 785–789.
(28) Frisch, M.J.; Trucks, G.W.; Schlegel, H.B.; Scuseria, G.E.; Robb, M.A.; Cheeseman, J.R.; Montgomery, J.A.; Vreven Jr., T.; Kudin, K.N.; Burant, J.C.; Millam, J.M.; Iyengar, S.S.; Tomasi, J.; Barone, V.; Mennucci, B.; Cossi, M.; Scalmani, G.; Rega, N.; Petersson, G.A.; Nakatsuji, H.; Hada, M.; Ehara, M.; Toyota, K.; Fukuda, R.; Hasegawa, J.; Ishida, M.; Nakajima, T.; Honda, Y.; Kitao, O.; Nakai, H.; Klene, M.; Li, X.; Knox, J.E.; Hratchian, H.P.; Cross, J.B.; Adamo, C.; Jaramillo, J.; Gomperts, R.; Stratmann, R.E.; Yazyev, O.; Austin, A.J.; Cammi, R.; Pomelli, C.; Ochterski, J.W.; Ayala, P.Y.; Morokuma, K.; Voth, G.A.; Salvador, P.; Dannenberg, J.J.; Zakrzewski, V.G.; Dapprich, S.; Daniels, A.D.; Strain, M.C.; Farkas, O.; Malick, D.K.; Rabuck, A.D.; Raghavachari, K.; Foresman, J.B.; Ortiz, J.V.; Cui, Q.; Baboul, A.G.; Clifford, S.; Cioslowski, J.; Stefanov, B.B.; Liu, G.; Liashenko, A.; Piskorz, P.; Komaromi, I.; Martin, R.L.; Fox, D.J.; Keith, T.; Al-Laham, M.A.; Peng, C.Y.; Nanayakkara, A.; Challacombe, M.; Gill, P.M.W.; Johnson, B.; Chen, W.; Wong, M.W.; Gonzalez, C.; Pople, J.A. *Gaussian 03, Revision C.01*; Gaussian, Inc. Wallingford, CT, 2004.
(29) Chattaraj, P.K.; Sarkar, U.; Roy, D.R. *Chem. Rev.* **2006**, *106*, 2065–2091.
(30) Job, P. *Ann. Chim.* **1928**, *9*, 113–203.
(31) Chou, P.T.; Wu, G.R.; Wei, C.Y.; Cheng, C.C.; Chang, C.P.; Hung, F.T. *J. Phys. Chem. B.* **2000**, *104*, 7818–7829.
(32) Fielding, L. *Tetrahedron* **2000**, *56*, 6151–6170.